Particle-in-cell investigation on the resonant absorption of a plasma surface wave

Lan Chao-Hui(蓝朝晖)[a)†] and Hu Xi-Wei(胡希伟)[b)]

[a)] *Institute of Fluid Physics, China Academy of Engineering Physics, Mianyang* 621900, *China*

[b)] *College of Electrical and Electronic Engineering, Huazhong University of Science and Technology, Wuhan* 430074, *China*

(Received 9 March 2011; revised manuscript received 12 May 2011)

The resonant absorption of a plasma surface wave is supposed to be an important and efficient mechanism of power deposition for a surface wave plasma source. In this paper, by using the particle-in-cell method and Monte Carlo simulation, the resonance absorption mechanism is investigated. Simulation results demonstrate the existence of surface wave resonance and show the high efficiency of heating electrons. The positions of resonant points, the resonance width and the spatio-temporal evolution of the resonant electric field are presented, which accord well with the theoretical results. The paper also discusses the effect of pressure on the resonance electric field and the plasma density.

Keywords: particle-in-cell simulation, plasma surface wave, resonant absorption

PACS: 52.65.Rr, 52.65.Pp, 52.50.Sw **DOI:** 10.1088/1674-1056/20/10/105202

1. Introduction

Surface wave plasma (SWP) sources have been heavily investigated in recent decades because of their potential industrial applications. SWP is sustained by the fields of 2.45-GHz microwaves propagating along a plasma-dielectric interface under the condition of an electron density higher than the cutoff plasma density.[1] One of the advantages of SWP sources is that they can be easily enlarged to diameters larger than 0.6 m or areas larger than 0.5 m^2 (0.5 m×1 m) and maintain good spatial uniformity and high density ($n_e \approx 10^{11}$ cm^{-3} $\sim 10^{13}$ cm^{-3}) of plasma at a wide-range gas pressure of 0.1 mTorr∼1.6 Torr (1 Torr=1.33322×10^2 Pa) without the use of external electrodes (avoiding pollution) and magnets.

Although several SWP sources of different configurations have been successfully developed,[2−13] some critical physical mechanisms are still not very clear, e.g. the power deposition mechanism. There are two possible mechanisms of power deposition in SWP that have already discovered and studied by researchers. One is through collision (i.e. Ohm heating) and the other is microwave local resonant absorption. As an effective heating mechanism of non-magnetic and non-collision plasma, local resonant absorption has been investigated for many years, but this phenomenon has been observed in experiments only recently.[14] Since the power deposition of microwaves is entirely restricted in a very thin area below the dielectric window, the resonant point is very close to the plasma boundary, at a distance shorter or of the same order of magnitude as the available experimental space resolution. So it is difficult to distinguish resonance spatially by existing diagnostic tools. Ghanashev *et al.* in their experiments have demonstrated that the electron density at the resonant point is just equal to the corresponding critical density. Although local resonance can be proved by those experiments, whether or not there exists local resonant absorption in SWP source still confuses researchers, because in those peculiarly designed experiments the resonant point is far from dielectric window, which is very different from real discharge conditions.

Local resonant absorption is concerned with the capability and efficiency of power deposition, especially when SWP sources are working at low gas pressures (i.e. less than 10 Pa) and as a result a non-collision mechanism dominates the heating of electrons. The particle-in-cell (PIC) method[15] is widely used by the plasma physics community to investigate plasma nonlinear and kinetic problems. After embedding the Monte Carlo method, PIC can simulate plasma generation and vanishing due to collision, but a single PIC cannot. Because of the difficulty of experimental diagnosis, in this paper, we adopt PIC plus Monte Carlo simulation to study the local resonance absorption of an SWP source.

†Corresponding author. E-mail: lanchaohui@163.com

© 2011 Chinese Physical Society and IOP Publishing Ltd

2. Physical model

Electron plasma resonance is a local enhancement of the electric field in inhomogeneous microwave plasma at positions where the local electron density n_e is equal to the cutoff density n_c (or in other words, the local electron plasma frequency ω_p is equal to the wave frequency ω).[14] The enhanced component is the one parallel to the electron density gradient (the z direction below). Figure 1 shows the variations of electron density, plasma permittivity and microwave intensity near the resonance point. The resulting microwave field is well described by the expression[16]

$$E_z(z,t) = \mathrm{Re}\left(\frac{E_{z0}\,\mathrm{e}^{-\mathrm{i}\,\omega t}}{1+\mathrm{i}\,(z-z_{\mathrm{res}})/\Delta}\right), \tag{1}$$

where $\Delta = (v/\omega)\,n_c\,(\mathrm{d}n_e/\mathrm{d}z)^{-1}$ is the resonance width, v is the collision frequency between electrons and neutral particles, and E_z is the microwave intensity at the resonance point z_{res}.

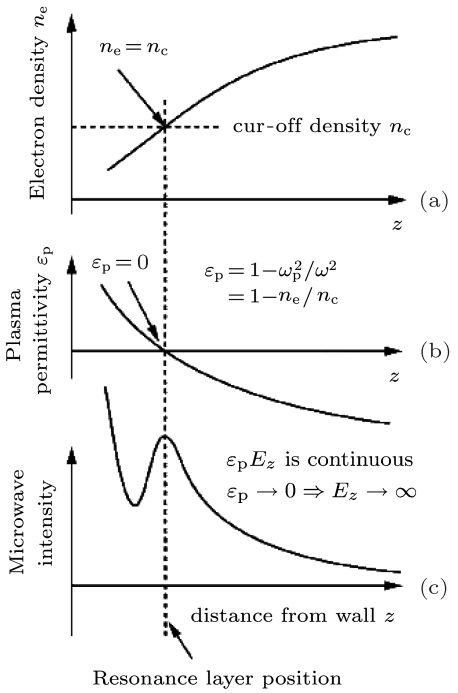


Fig. 1. The local electron plasma resonance layer with profiles of (a) the local plasma density, (b) the local plasma permittivity, and (c) the local electric field intensity.

The plasma surface wave (PSW) is electromagnetic and the electric field plays a main role in heating electrons, because the force acting on electrons by the magnetic field is too small as compared with the electrical force and can be neglected. After building up the propagation of the PSW, the electric field of the PSW is evanescent on both sides of the plasma and dielectric window. The electric field penetration depth can be roughly described by

$$\delta = \frac{c}{\omega\,\mathrm{Im}\left(\sqrt{\varepsilon_p}\right)}, \tag{2}$$

where ε_p is the plasma permittivity

$$\varepsilon_p = 1 - \frac{\omega_p^2}{\omega\,(\omega+\mathrm{i}\,v)}. \tag{3}$$

For a low-pressure SWP source operated at $f = 2.45$ GHz, the plasma density is typically larger than the cutoff density $n_c = 7.4\times10^{10}$ cm^{-3} within several centimeters distance from dielectric window. Hence the plasma frequency ω_p is much higher than both the wave frequency ω and collision frequency v. Accordingly Eq. (2) can be simplified to $\delta \sim c/\omega_p$, resulting in a penetration depth shorter than 1 cm$\sim$2 cm. For example, when $n_e = 10^{12}$ m^{-3}, δ is about 0.53 cm.

In order to study the local resonance by using PIC code, we make the following assumptions. (i) The initial plasma is uniform spatially and the density is 2.0×10^{10} cm^{-3}, which is far below the cutoff density. (ii) The working gas is argon and collision includes elastic collision, excitation and ionization. (iii) The electric field with the same profile as the surface wave is expressed as

$$E_z(d,t) = A\exp(-d/l)\cos(2\pi f t), \tag{4}$$

where d is the distance to the plasma-dielectric interface, l is the microwave penetration depth and A is the electric field intensity. Since we consider the variations of electric field and plasma parameters only in the perpendicular direction (i.e. z direction), the calculation model is one-dimensional. Here, one should note that the electric field is external but not self-consistently generated by radiation of antenna and surface wave excitation, otherwise the calculation model must be two- or three-dimensional. However, the local resonance absorption of the PSW can also be investigated by adjusting the electric field and making the profile approximately the same as the self-consistent surface wave. In our calculations, the parameters that determine the electric field profile are fixed to $l = 4$ mm and $A = 32500$ V/m. The intensity of the electric field is as much as that of a surface wave excited by microwave deposition power of 1200 W in a 44 cm$\times$22 cm area.

Figure 2 shows the physical model of PIC simulation. The total spatial length is 10 cm, the left and right sides are both absorption boundary conditions for particles. The time step is set to be 1.33×10^{-11} s, the cell size is 0.05 mm, the initial ratio of particle to cell number is 50 and the particles we adopted have

true charge-mass ratios. The initial plasma is uniform and the temperatures of the electrons and ions are 4 eV and 0.05 eV, respectively. Argon gas pressure is set to be 0.6 Torr and the temperature is 0.03 eV.

In the Monte Carlo course, the following collision processes are considered: elastic collision, excitation collision, ionization collision, charge exchange collision and scattering collision. For more details, see Ref. [15]. Thus under the excitation of exponential decay electric field, it is reasonable to expect that plasma density within excitation zone would increase rapidly and exceed the cutoff density.

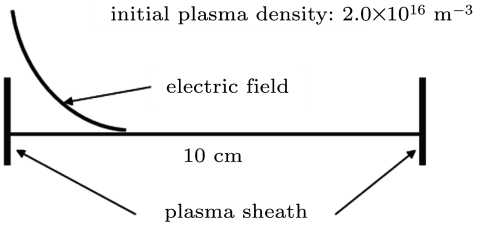


Fig. 2. Physical model.

3. Results and discussion

The direct method for the increase of ion number is to raise the collision ionization rate, which intrinsically needs to heat electrons. In the SWP, Ohm heating and resonant heating coexist, but their significance is different at different moments. Figure 3 shows the temporal evolution curve of the electron super-particle number. On the whole, the curve can be divided into three parts. The first part lies in the range of 0 ns–150 ns, in which the plasma density increases slowly under the excitation of an external electric field. So this is an Ohmic heating phase. The second part lies in the range of 150 ns–280 ns, in which plasma density increases rapidly. Obviously, in this phase two heating mechanisms coexist, but the resonant heating achieves complete dominance. Finally, the third part lies after 280 ns, in which the increasing rate of plasma density slows down. In this phase, we think that two heating mechanisms also coexist but Ohmic heating regains dominance. Comparing the three phases, we can see that Ohmic heating is much slower than resonant heating. Namely, the efficiency of electron heating through electric field acceleration and then collision with neutral particles to change directions is much lower than through resonant heating.

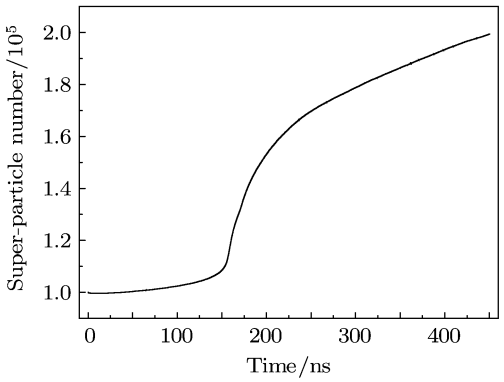


Fig. 3. Temporal evolution of super-particle number.

In order to further reveal the dominant role of resonance on electron heating at the second phase mentioned above, figure 4 shows the distributions of electron temperatures at different moments. At 267 ns, two peaks of electron temperature can be found in the excitation zone and each peak is supposed to be a resonance point. The reason will be further discussed in the following paragraph. Electron plasma resonance always causes the electron temperature to rise at first and then makes the plasma density rise through the collision of electrons with neutral particles. The temperature in the excitation zone locally reaches more than 6 eV by resonance in a very short time, and decreases slowly to 4 eV after plasma density mostly increasing to higher than the cutoff density in phase three. The electron temperature far away from excitation zone also decreases from the initial value due to loss of energy by collisions.

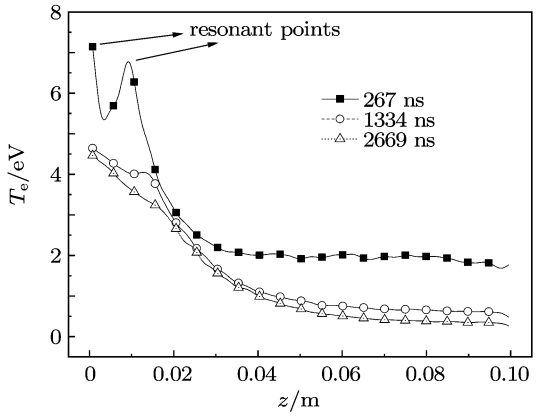


Fig. 4. Spatial distributions of electron temperature at different moments.

Distributions of electron density, electric field in plasma and input electric field at 267 ns are shown in Fig. 5. Plasma density within the excitation zone mostly has exceeded the cutoff density. Only near the left sheath boundary and right low electric field

area is the plasma density lower than the cutoff density. Therefore, it can be found that there are two resonant peaks of the electric field, corresponding to two different resonant points. For an actual SWP source, plasma of a density higher than the cutoff density would be thicker than 2 cm, so the second resonant point would not appear. However, the resonant point of the left side would exist at the times as long as the nearby plasma density is higher than the cutoff density. Due to the effect of the plasma sheath, the plasma density near the dielectric boundary is very low, hence the positive gradient of plasma density needed for resonance (i.e. Fig. 1(a)) is always satisfied.

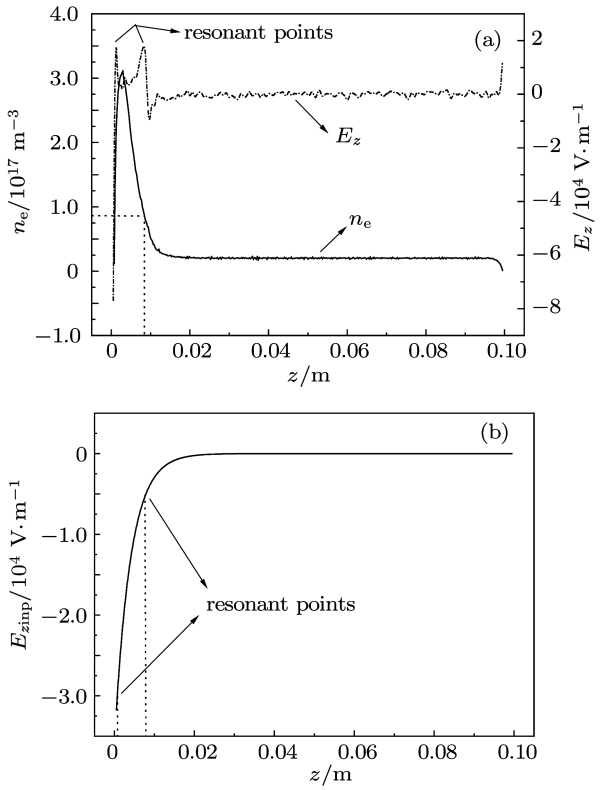


Fig. 5. Distributions of (a) electron density, electric field in plasma and (b) input electric field at 267 ns.

Figure 6 depicts the temporal evolution of the electric field at the resonant point, which comes from Eq. (1). It can be easily shown that an electric field with time/space dependence can change the velocity (and eventually accelerated) of only those electrons running down the density gradient (i.e. towards the plasma sheath boundary). This is due to the traveling-wave character (Fig. 6) of the local plasma resonance from Eq. (1), which, after Fourier transformation, turns out to be a superposition only of the plane waves travelling to the plasma boundary. Such waves can accelerate an electron flying synchronously with them in a Landau damping-like interaction, while electrons running the opposite way (to the plasma) remain unaffected. For the accelerated electrons, only those with relatively low energies could eventually be reflected back to the plasma from the barrier of the sheath potential. High-energy electrons directed to the plasma are similar to the secondary electrons generated when the electrons accelerated to high energies in the resonance region reflect back from the sheath boundary.

Equation (1) (or Fig. 6) is merely a theoretical result, as far as we know, it has not been validated by any experiments up to now. Figure 7 is our PIC simulation result, showing the spatial and temporal evolution of electric field in the excitation region. Primarily, we are concerned with the left resonant point, but it is very close to the left sheath boundary and difficult to distinguish. So we turn our attention to the right resonant point for a while. Comparing the curves at different moments (i.e. different phases) in Figs. 6 and 7, one can see that the simulated evolution of the electric field at the resonant point perfectly matches the theoretical result, just the directions are opposite. The reason for the different directions of wave travelling is due to the opposite density gradients of plasma, which are shown in Fig. 5(a) and Fig. 1.

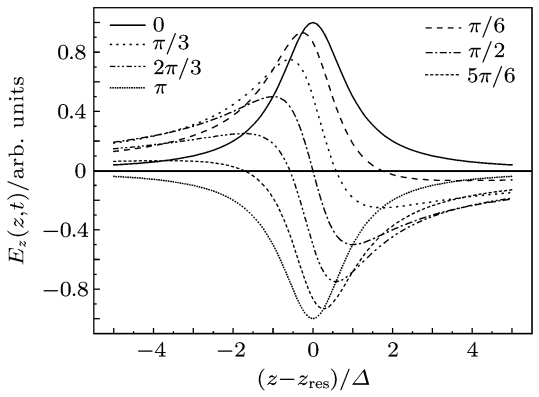


Fig. 6. Spatial and temporal evolution of the electric field in the local electron plasma resonance, from Eq. (1) demonstrating travelling-wave behavior directed towards the wall.

The density gradient of plasma at right resonant point (i.e. $z \approx 0.9$ cm) can be measured from Fig. 5(a) and is about 2.0×10^{17} m^{-3}/0.009 m. Substituting gas pressure $p = 0.6$ Torr and electron temperature $T_e = 4$ eV into formula $\nu_{en} = 1.52 \times 10^7 p\,[\mathrm{Pa}]\sqrt{T_e[\mathrm{eV}]}$, the electron collision frequency ν_{en} is 2.43×10^9 s^{-1}. Finally, the resonance width can be calculated and is about $\Delta = 0.53$ mm. This result agrees quite well with that shown in Fig. 7. Now we turn our attention

to the left resonant point again. One should note that at the same moment, the phase of the resonant electric field of the left resonant point is opposite to that of the right one, hence the electric field in the local resonance would be covered by the sheath electric field. That is the reason why we cannot observe the left resonant electric field from Fig. 7. However, the left resonance width can be estimated from both Fig. 5 and the calculated resonance width of the right one. Through comparison of the two peaks of the resonant electric field in Fig. 5, we obtain the left resonance width being about 1/5 of the right resonance width, i.e. 0.1 mm. Considering that the average plasma density near the dielectric flat in an actual SWP source working at 0.6 Torr could be more than 3.0×10^{17} m^{-3}, it is reasonable to believe that the resonance width would be less than 0.1 mm.

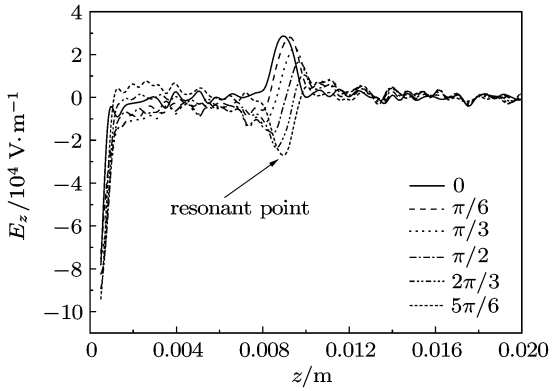


Fig. 7. Spatial and temporal evolutions of electric field from PIC simulation.

Aforementioned simulation results have demonstrated the possibility of maintaining discharge through resonance absorption of PSW. However we found that it does not always occur for a wide range of pressures. Figure 8 gives the variations of spatial distributions of electron density and electric field at different pressures. Here, in order to speed up the calculations, the initial uniform plasma density is set to 7.0×10^{16} m^{-3}, slightly smaller than the cutoff density. One can see that for a relatively high pressure (e.g. 0.05 Torr), the surface wave can easily generate plasma, the density of which is higher than the cutoff density through resonance absorption. However, when the pressure decreases, the plasma density gradient gets smaller and the resonant point moves backwards. Although a small density gradient can broaden the resonance width and as a result enhance the absorption of PSW, because the resonant point is far from the dielectric boundary and the input electric field decreases with distance, the amplitude of the excited resonance electric field would become very small, leading to a weak capability of plasma generation. One can further deduce that for a low enough pressure (e.g. below 0.1 mTorr), the resonant absorption of PSW cannot maintain discharging.

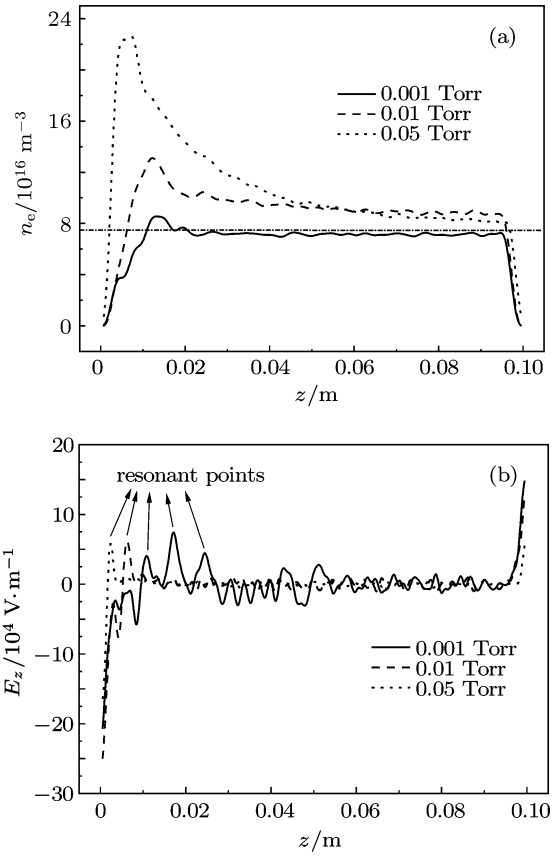


Fig. 8. Spatial distributions of electron density (a) and electric field (b) for different gas pressures (at 2660 ns).

4. Conclusion

In this paper, we have simulated the resonant absorption of a plasma surface wave using particle-in-cell plus Monte Carlo algorithm. The spatio-temporal variations of plasma parameters under the excitation of an exponentially decayed electric field have been presented. The simulation results show the structure of resonant electric field and the width of resonance, which accord well with the theoretical results. We also found that plasma surface wave resonance is a very effect mechanism for power deposition, but the resonant point in the surface plasma source is quite close to the dielectric boundary and leads to a relatively low deposition efficiency when the plasma density is too high. Since surface wave resonance is relevant to the gradient of plasma density, at low pressure, resonance absorption may be a dominant mechanism in power deposition.

References

[1] Sugai H, Ghanashev I and Nagatsu M 1998 *Plasma Sources Sci. Technol.* **7** 192

[2] Ghanashev I, Nagatsu M, Morita S and Sugai H 1998 *J. Vac. Sci. Technol.* A **16** 1537

[3] Nagatsu M, Morita S, Ghanashev I, Ito A, Toyoda N and Sugai H J 2000 *Physica* D: *Appl. Phys.* **33** 1143

[4] Ghanashev I and Sugai H 2000 *Phys. Plasmas* **7** 3051

[5] Ganashev I, Nagatsu M and Sugai H 1997 *Jpn. J. Appl. Phys.* **36** 337

[6] Wu T J, Guan W J and Tsai C M 2001 *Phys. Plasma* **8** 3195

[7] Nagatsu M, Ghanashev I and Sugai H 1998 *Plasma Sources Sci. Technol.* **7** 230

[8] Nagatsu M, Naito K, Ogino A and Nanko S 2006 *Plasma Sources Sci. Technol.* **15** 37

[9] Lan C H, Hu X W, Jiang Z H and Liu M H 2010 *Acta Phys. Sin.* **59** 4093 (in Chinese)

[10] Ou Q R and Liang R Q 2002 *Vacuum and Low Temperature* **8** 28 (in Chinese)

[11] Zhan R J, Wu C F, Wen X H, Zhu X D and Zhou H Y 2001 *Vac. Sci. Technol.* **21** 30 (in Chinese)

[12] Liang Y Z, Ou Q R, Liang B and Liang R Q 2008 *Chin. Phys. Lett.* **25** 1761

[13] Chen Z Q, Zhou P Q, Chen W, Lan C H, Liu M H and Hu X W 2008 *Plasma Sci. Technol.* **10** 655

[14] Ganashev I, Sugai H, Morita S and Toyoda N 1999 *Plasma Sources Sci. Technol.* **8** 363

[15] Birdsall C K 1991 *IEEE Trans. Plasma Sci.* **19** 65

[16] Ginzburg V 1965 *The Propagation of Electromagnetic Waves in Plasmas* (London: Pergamon Press)